Materials Science and Technology

ISSN: 0267-0836 (Print) 1743-2847 (Online) Journal homepage: http://www.tandfonline.com/loi/ymst20

Microstructure and microhardness of pearlitic steel after laser shock processing and annealing

Y. Xiong, T. T. He, L. You, P. Y. Li, L. F. Chen, F. Z. Ren & A. A. Volinsky

To cite this article: Y. Xiong, T. T. He, L. You, P. Y. Li, L. F. Chen, F. Z. Ren & A. A. Volinsky (2015) Microstructure and microhardness of pearlitic steel after laser shock processing and annealing, Materials Science and Technology, 31:15, 1825-1831, DOI: 10.1179/1743284715Y.0000000020

To link to this article: http://dx.doi.org/10.1179/1743284715Y.0000000020

Published online: 25 Apr 2015.

Microstructure and microhardness of pearlitic steel after laser shock processing and annealing

Y. Xiong*[1,2], T. T. He[3], L. You[1,2], P. Y. Li[1], L. F. Chen[1], F. Z. Ren[1,2] and A. A. Volinsky[4]

The microstructure evolution of the high carbon pearlitic steel after laser shock processing (LSP) with different laser pulse energy and high temperature annealing was investigated. After LSP, the cementite lamella were bent, fractured and broken into granules. Fragmentation and dissolution of the cementite lamella were enhanced by increasing the laser pulse energy. Results show that the ferrite lattice parameter increased due to carbon atom dissolution in the ferrite matrix, and the corresponding ferrite X-ray diffraction peaks shifted significantly towards the smaller diffraction angles. After annealing at 650°C for 30 min, an ultrafine duplex microstructure (ferrite + cementite) was formed on the surface. After LSP with a high energy, equiaxed ferrite grains were refined to 400 nm and the cementite lamella were fully spheroidised with the particle diameter of ~150 nm. The corresponding grain size of ferrite and cementite under low pulse energy was 500 and 300 nm respectively. After annealing, the ferrite peaks significantly shifted towards the higher diffraction angles, and the ferrite lattice parameter decreased. The microhardness initially increases after LSP and then slightly decreases after subsequent annealing but remained higher than without LSP.

Keywords: Laser shock processing, High carbon pearlitic steel, Microstructure, Microhardness

Introduction

Ultrafine grained steels belong to a class of high performance structural materials and have recently attracted significant attentions from researchers and developers. Since high carbon steels are widely used as materials for tools and dies due to a combination of adequate strength and wear resistance, enhancement of their toughness and ductility will be beneficial for extended applications. One possible way for high carbon steels to achieve excellent overall performance is the grain refinement process during industrial production. In recent years, it has also been noticed that ultrafine microduplex structure (ferrite+cementite) with excellent mechanical properties and superplasticity has been produced in high carbon pearlitic steel through severe plastic deformation (SPD), such as severe cold rolling and annealing,[1,2] and equal channel angular pressing.[3] However, the strain rate of SPD processing is quite low ($<10\ s^{-1}$), which leads to large deformation resistance. Thus, this method is currently confined to laboratory experiments due to the special advanced equipment requirements.

As a new surface processing technology, laser shock processing (LSP) can produce ultrahigh strain rate up to 10^6–$10^7\ s^{-1}$. The generated shock wave can produce SPD, as well as deep compressive residual stresses of several hundreds of MPa by exposing metallic samples to high power density and short pulse laser beam. Previous studies have shown that the grain size of the alloy top layer can be refined to the nanoscale[4] and even become amorphous[5], with the gradient structures formed in the top layer.[6] Previous research also suggested that LSP can improve fatigue life,[7] corrosion,[8] wear resistance[9] and other mechanical properties[10,11] of metals and alloys. Up to now, LSP technique has very good application prospects in the aerospace sector and the automobile manufacturing due to its characteristics of simple, flexible and easy to realise automation control. Moreover, regions inaccessible to shot peening, such as small fillets and notches, can be quickly and effectively treated by LSP. The samples with larger surfaces can be treated in the form of overlapping multipass LSP. Although essentially a surface modification technique, increasing the laser spot size and/or overlapping LSP traverses can increase the affected area, thereby increasing the potential applications of this technique.

Many efforts have been devoted to study the microstructure and mechanical properties of aluminium alloys, magnesium, titanium, copper and low carbon

[1]School of Materials Science and Engineering, Henan University of Science and Technology, Luoyang 471003, China
[2]Collaborative Innovation Center of Nonferrous Metals, Henan Province, Luoyang 471003, China
[3]Institute of Metals Research, Chinese Academy of Sciences, Shenyang 110016, China
[4]Department of Mechanical Engineering, University of South Florida, Tampa, FL 33620, USA

*Corresponding author, email xy_hbdy@163.com

Published by Maney on behalf of the Institute
Received 12 November 2014; accepted 29 January 2015
DOI 10.1179/1743284715Y.0000000020

steel enhanced by the LSP, primarily confined to room temperature. Only a few studies have focused on the microstructure and mechanical properties under high temperatures after LSP. Ren *et al.* investigated the microstructure evolution of the aluminium alloy processed by LSP under high temperature annealing and explored the strengthening mechanisms.[12,13] The mechanical properties of stainless steels under the same conditions were also investigated.[14] Ye *et al.*[15] focused on the microstructure of NiTi alloys processed by LSP under high temperature annealing. However, only a few reports have studied the microstructure and mechanical properties of carbon steels under high temperature annealing after LSP. The aim of the paper is to study the microstructure evolution of high carbon pearlitic steel by LSP with different laser pulse energy under high temperature annealing and to provide useful insights into the controllable preparation of the gradient structures in the high carbon steels.

Experimental

The commercial Fe–0.8 wt-%C steel ingots, 20 mm in diameter, 2 mm high, were selected for the present research. Those ingots were initially homogenised for 30 min at 1000°C before they were introduced into a salt bath, and heated at 600°C for 60 min, followed by air cooling to room temperature to ensure the full evolution of pearlite. Then, these ingots were mechanically ground and polished, followed by cleaning in the deionised water. Ultrasound cleaning in ethanol was used to degrease the sample surface, and finally, LSP was conducted shortly after the sample preparation.

During the LSP process, the shock waves were induced by the Nd:glass laser with a wavelength of 1064 nm and 10 ns pulse. The laser spot diameter was 3 mm, and the overlapping rate of the laser spot was 50%. Water with a thickness of $\sim$1 mm was used as the transparent confining layer, and the aluminium foil with a thickness of 0.1 mm was used as an absorbing layer to protect the specimen surface from the thermal effects. The laser energy was either 2 or 6 J. The LSP shock region, along with the scan direction of the sample, can be found in Ref. 13. After LSP, the treated samples were heated to 650°C for 30 min, followed by air cooling to room temperature. The annealing temperature is selected based on our previous studies[16,17] and other references,[18,19] because the spheroidisation of cementite lamella after severe deformation can be accelerated at the temperature of 650°C for 30 min.

The metallographic structure of the samples obtained by LSP and annealing was observed with the field emission scanning electron microscope (QUANTA FEG 650) after etching in the 4% Nital solution at room temperature. The microstructure evolution of the treated samples' surface after LSP and annealing was characterised using JEOL JEM-2100 high resolution transmission electron microscope (TEM) operated at 200 kV. TEM foils were initially prepared without straining, followed by grinding to $\sim$30 μm thickness, and further thinned by the twin jet electropolishing. The X-ray diffraction (XRD) experiments were carried out on a D8 ADVANCE X-ray diffractometer. The tube voltage and current were 35 kV and 40 mA respectively. The tube anode was Cu $K_{\alpha 1}$ ($\lambda = 0.15406$ nm), and the width of the receiving slit was 2 mm. The position of each reflection was determined using the curve width at half maximum method.[20] The final lattice parameter of ferrite was obtained by data treatment, including extrapolation and the least squares method. The microhardness of the laser processed regions was measured by the MH-3 Vickers microhardness tester (200 g load, 10 s holding time). An average microhardness value was determined based on five indentation measurements.

Results and discussion

Figure 1 shows the microstructure of the as received Fe–0.8 wt-%C steel. It can be seen that the initial microstructure was full pearlite. The thickness of the cementite lamellae is $\sim$30 nm, and the average lamellae spacing is $\sim$150 nm, as seen in Fig. 1*b*.

Figure 2*a* and *b* shows the microstructure of the Fe–0.8 wt-%C steel annealed at 650°C for 30 min without LSP. Compared with the initial microstructure, there are no obvious changes in the lamellae spacing after annealing, but fracture of the cementite lamellae can be found in the local region, indicating the tendency of spheroidising of the cementite lamellae. Figure 2*c–f* shows the microstructure of the Fe–0.8 wt-%C steel after LSP. After LSP with a low energy of 2 J, the cementite lamella are bent and fractured, and some cementite lamella are broken into smaller ones, as seen in Fig. 2*c*. After LSP with a high energy of 6 J, severe deformation is observed in the lamella and a large amount of cementite lamella are

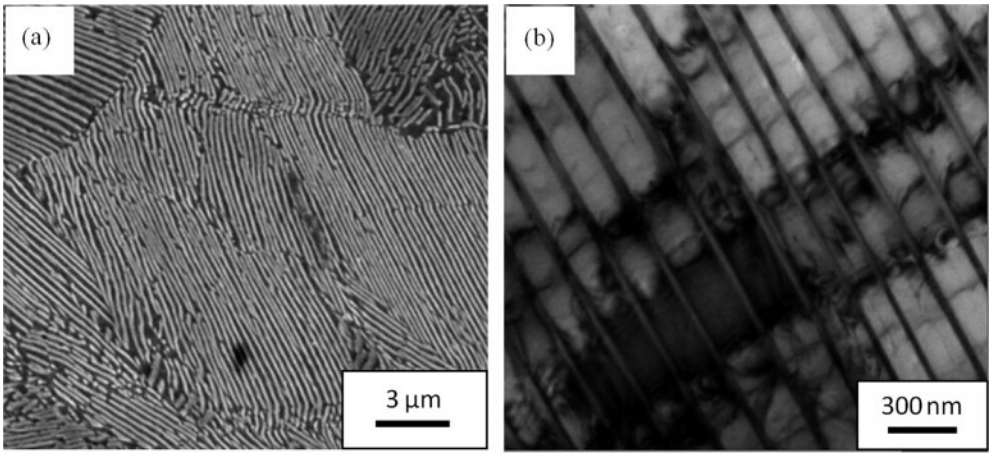

1 Pearlite microstructure of high carbon steel: *a* SEM; *b* TEM

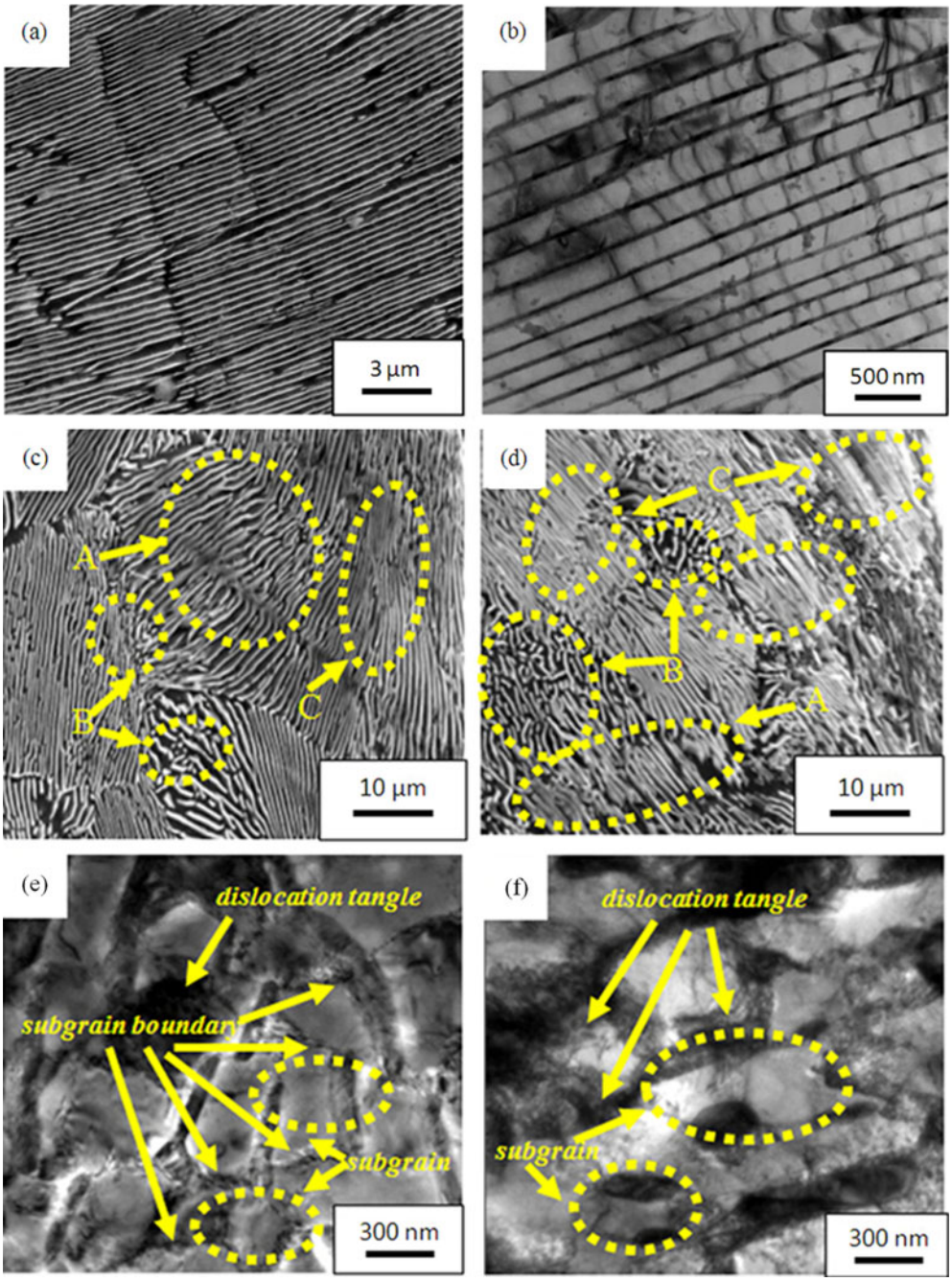

2 Microstructure of Fe–0·8 wt-%C steel annealed at 650°C for 30 min without LSP: *a* SEM; *b* TEM; SEM images of Fe–0·8 wt-%C steel processed with different laser pulse energies: *c* 2 J; *d* 6 J; TEM images of Fe–0·8 wt-%C steel processed with different laser pulse energies: *e* 2 J; *f* 6 J

fractured into smaller ones. The interlamellar spacing of cementite apparently decreases, regional lamellars fracture periodically, and the deformation intensifies, compared with the low LSP energy, as seen in Fig. 2*d*. This is mainly because each pearlite colony has distinct stress state, leading to defferent deformation from others, due to their defferent orientation with respect to the LSP impact derection. When the angle between pearlite colony and deformation derection becomes much larger, cementite lamellar undergoes bending deformation (A area of Fig. 2*c* and *d*), may fracture (B area of Fig. 2*c* and *d*), and even dissolves as the pulse energy further increases. The interlamellar spacing of cementite decreases as the angle became smaller (seen in area C of Fig. 2*c* and *d*). Figure 2*e* and *f* shows TEM images of the samples after LSP with laser pulse energies of 2 and 6 J respectively. After LSP with a laser pulse energy of 2 J, more dislocations are formed and dislocation pileups contribute to the formation of dislocation tangles and dense dislocation cells, then the lamella are fractured in the shape of a short bar, finally leading to the formation of subgrains with a grain size of ~400 nm, as seen in Fig. 2*e*. After high energy LSP, subgrains with a grain size of ~300 nm are developed as the result of the further increase in dislocation density responsible for dislocation tangles. The degree of fragmentation is much higher than under low pulse energy, and the initial arrangement of the cementite lamella can be observed, as seen in Fig. 2*f*.

Figure 3 shows the SEM images of the Fe–0·8 wt-%C steel annealed at 650°C for 30 min after LSP. It can be

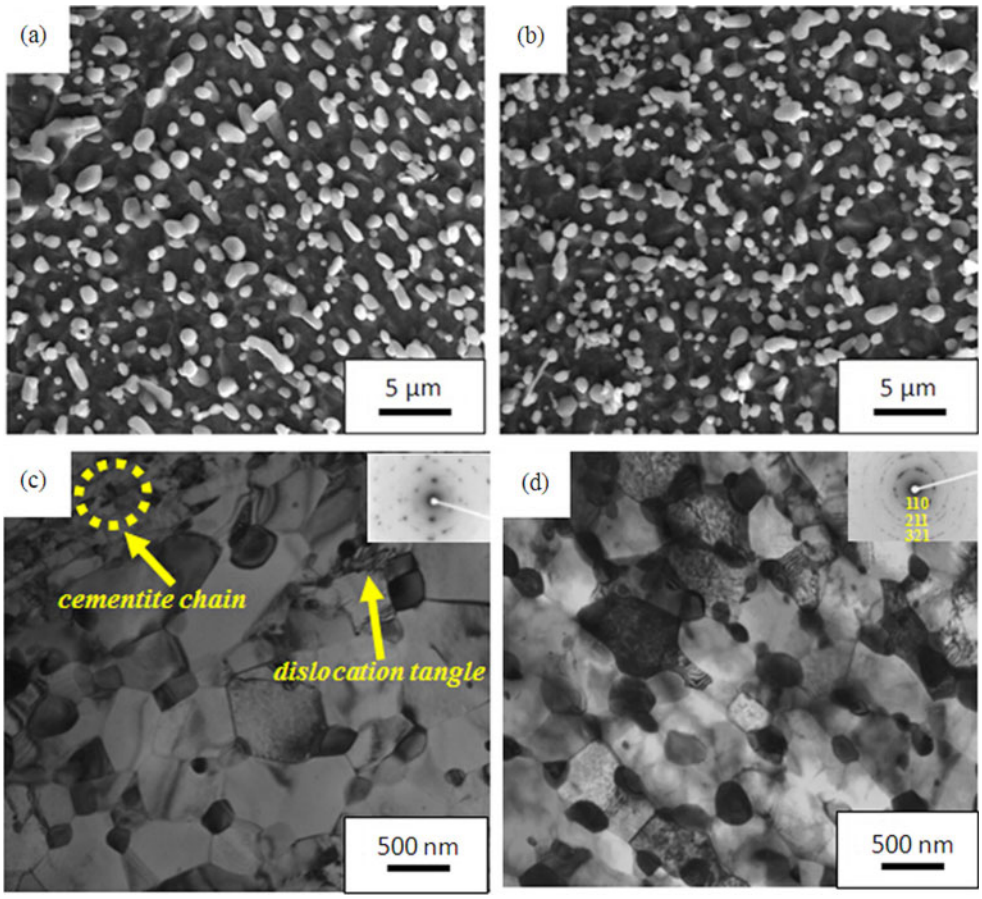

3 SEM images of Fe–0·8 wt-%C steel annealed at 650°C for 30 min after LSP with different laser pulse energies: *a* 2 J; *b* 6 J; TEM images of Fe–0·8 wt-%C steel annealed at 650°C for 30 min after LSP with different laser pulse energies: *c* 2 J; *d* 6 J

seen that cementite lamella spheroidised completely after annealing treatment, and the diameter of the fully spheroidised cementite under low pulse energy is obviously larger than under high energy. After LSP with a low energy of 2 J, the diameter is ~200–400 nm in Fig. 3*a*. As the energy increases to 6 J, the diameter declines to ~100–300 nm, as seen in Fig. 3*b*. Microstruture varies due to the extent of deformation performed by cementite. The degree of fragmentation of cementite intensifies from low to high pulse energy, leading to the higher extent of spheroidisation and smaller diameter of cementite under high pulse energy. During the following annealing process, the dislocation density gradually decreased due to the ferrite recovery and recrystallisation. The binding energy of Fe and C atoms is higher than that of the C atoms with dislocations. Thus, supersaturated C atoms reserved in dislocations precipitated from the ferritic grains in the form of the nanoscale cementite particles.[21,22] However, according to the Gibbs–Thomson effect, larger cementite particles are formed at the grain boundaries due to the cementite lamella fracture and spheroidisation.

Figure 3*c* and *d* shows TEM images of the Fe–0·8 wt-%C steel annealed at 650°C for 30 min after LSP with laser pulse energies of 2 and 6 J respectively. After the annealing treatment, pearlite lamella change into ultrafine duplex microstructure (ferrite + cementite). After 2 J in pulse energy, the diameter of ferrite is ~500 nm and cementite is ~200–300 nm. In addition, a small amount of dislocation tangles and cementite chains is observed in some local areas. After LSP with a higher 6 J energy, the ferrite grains are fully equiaxed with the grain size of ~400 nm, and the fully spherised particles of cementite are dispersively distributed on the ferrite grain boundaries, with diameters of 100–250 nm. A small amount of cementite particles with a diameter of 50 nm arises in ferrite grains due to the reprecipitation of nanoscale cementite from supersaturated ferrite under annealing.[23]

The corresponding selected area electron diffraction (SAED) profiles are located at the top right corner of the images in Fig. 3. The diffraction spots of ferrite are discontinuous after low energy LSP, as seen in Fig. 3*c*. This confirms the existence of low angle grain boundaries. However, in Fig. 3*d*, the SAED pattern with an aperture size of 2.5 μm shows a clear and uniformly continuous diffraction ring pattern, compared with Fig. 3*c*. Indexes corresponding to the three clear rings are marked on the diffraction pattern, which corresponded to (1 1 0), (2 1 1) and (3 2 1) reflections of α-Fe in Fig. 3*d*. This suggests the presence of a large number of boundaries with high angle misorientation after LSP with a high energy of 6 J.[24]

XRD patterns of the Fe–0·8 wt-%C steel before and after LSP and high temperature annealing are shown in Fig. 4. Compared with the samples after LSP, the α-Fe peaks shift to smaller diffraction angles. The higher the LSP pulse energy, the more significant is the left shift of the ferrite peaks. Similar changes of the α-Fe lattice parameter are also reported in other studies of heavy cold rolled pearlitic steels.[25] Since LSP is a cold processing technique,[26,27] ultrahigh strain rate deformation

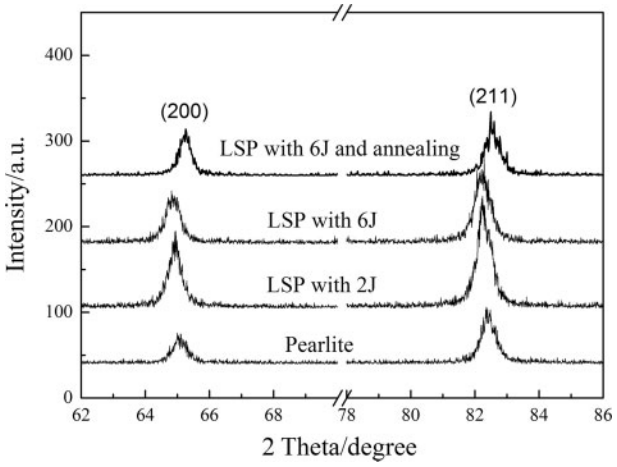

4 Changes of XRD peak positions of α-Fe in pearlitic Fe–0·8 wt-%C steel before and after LSP and high temperature annealing

introduced by the shock wave results in the cementite bending, kinking, fracturing and even dissolution to coordinate the ferrite deformation.

The original lattice parameter of α-Fe is 0·28664 nm in the Fe–0·8 wt-%C steel. After LSP with energies of 2 and 6 J, the lattice parameter of α-Fe increases to 0·28691 and 0·28712 nm respectively. According to Fasiska and Wagenblast,[28] the carbon content in the pearlite ferrite after different LSP pulse energies can be estimated based on the relationship between the lattice parameter and the carbon constant of α-Fe. Corresponding change of the carbon content in the α-Fe is estimated as 0·07% and 0·12% for the 2 and 6 J LSP respectively. In order to coordinate the deformation of the ferrite and the cementite during the ultrahigh strain rate deformation introduced by the shock wave, many dislocations are generated to provide diffusion path for C atoms, leading to the Cottrell atmosphere formation. This process can reduce the energy and lead to the cementite dissolution. The increase in the C content in the ferrite grains may be mainly due to the partial dissolution of the cementite lamella, resulting in the increase in C content to supersaturation in the deformed ferrite.[20,29]

After annealing at 650°C for 30 min, the ferrite peaks shift to larger diffraction angles. The lattice parameter of α-Fe is 0·28663 nm in the Fe–0·8 wt-%C steel, and the lattice parameter of α-Fe is nearly the same as before LSP. Owing to static recovery and recrystallisation during annealing, the dislocation density in the ferrite grains reduces. The supersaturated C atoms are reprecipitated from the ferrite in the form of cementite particles, which are dispersed in the ferrite at the nanometre scale. This is consistent with the results presented in Fig. 3*a* and *b*. In addition, similar phenomena were observed in Yang's reports on the warm deformation of eutectoid and hypereutectoid steels.[30,31]

Figure 5 shows the microhardness of the laser shocked area of Fe–0·8 wt-%C steel measured along the surface and the depth before and after annealing. It can be seen that microhardness increases with the LSP pulse energy, and microhardness in the impact centre is obviously improved compared with the corresponding values at the edge. This is because the stress induced by the shock wave has a Gaussian distribution due to the intrinsic character of the laser pulse energy.[29] In the impact centre, SPD occurred, so the microhardness is higher than in other regions. From Fig. 5*a*, after LSP with a laser pulse energy of 2 J, the microhardness increased by 9% from HV 300 (before LSP) to HV 328 in the impact centre. With the laser pulse energy increasing to 6 J, the microhardness is HV 344, which is a 14% increase compared with the samples without LSP. The hardness along the depth shows that the depths of the laser enhanced area are ~0·25 mm (2 J) and 0·4 mm (6 J), as seen in Fig. 5*b*. After annealing at 650°C for 30 min, the hardness of impact surface decreased to HV 316 and HV 330, compared with the untreated state, as shown in Fig.5*c*. This is because before annealing, LSP causes SPD; thus, the microstructure of the Fe–0·8 wt-%C steel results from the slip and pileup of high density dislocations, leading to dislocations pinning, as the pulse energy increased, and the ferrite subgrains resulted from the increase in dislocation density responsible for dislocation tangle. Therefore, after LSP, the surface microhardness increases mainly due to dislocation strengthening and fine grain strengthening. After heat treatment, dislocation density decreases tremendously, and simultaneously, the deformed cementite lamella spheroidised. The equiaxed ferrite grains are produced through static recovery and recrystallisation. Thus, the microhardness decreases after heat treatment. Although the microhardness after heat treatment is lower than after LSP, it is higher than without LSP.

The strain gradient from the surface to the deeper areas develops due to LSP, with different structure at various depths from the surface. Thus, a variety of resulting gradient deformation structures appear after annealing treatment. The next study will focus on the structural features and mechanical properties under various annealing temperature and holding time.

Conclusions

The effects of LSP on the microstructure evolution and microhardness of high carbon pearlitic steel at elevated temperature are investigated. The following conclusions can be drawn.

1. The plastic deformation of the sample with lamellar pearlite after LSP is mainly due to the deformation of the cementite lamella. Under the ultrahigh strain rate, the cementite is in the form of bent, kinked, fractured and even dissolved lamella to coordinate the deformation of the ferrite. The cementite dissolution increases with the laser pulse energy, leading to the ferrite lattice expansion. The ferrite peaks significantly shift towards the smaller diffraction angles.
2. After annealing at 650°C for 30 min, a submicrometre grain structure is formed on the surface. After LSP with the energy increasing from 2 to 6 J, the equiaxed ferrite grains are refined from 600 to 300 nm and the cementite lamella are fully spheroidised with the particle diameter decreasing from 150 to 100 nm. Meanwhile, the supersaturated C atoms are reprecipitated from the ferrite in the form of cementite particles with a grain size of ~50 nm. The ferrite peaks shift to larger diffraction angles, and the lattice parameter of α-Fe is nearly the same as that of the samples before LSP.

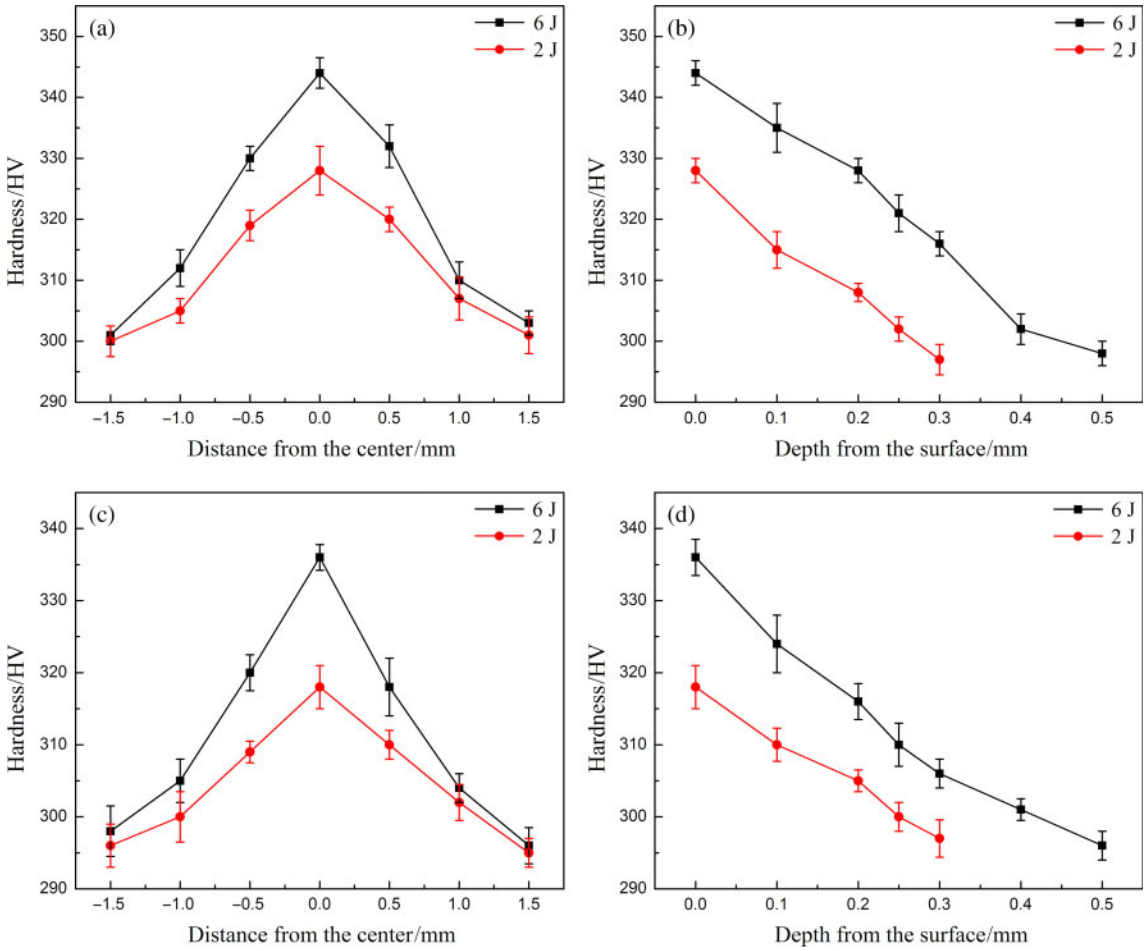

5 Microhardness of laser shocked area measured along surface and depth: *a*, *b* before annealing; *c*, *d* after annealing (red circles and black boxes indicate laser energies of 2 and 6 J respectively)

3. The surface microhardness increases after LSP due to dislocation strengthening and fine grain strengthening, then slightly decreases after subsequent annealing, but is still higher than the sample without LSP.

Acknowledgements

This work was supported by the National Natural Science Foundation of China (grant nos. 50801021 and 51201061), Program for the Young Key Teachers in the Henan Province (grant no. 2011GGJS-070) and the Henan Province Program for Science and Technology Innovation Excellent Talents (grant no. 144200510001).

References

1. T. Furuhara, T. Mizoguchi and T. Maki: 'Ultra-fine (α+θ) duplex structure formed by cold rolling and annealing of pearlite', *ISIJ Int.*, 2005, **45**, 392–398.
2. W. T. Fu, T. Furuhara and T. Maki: 'Effect of Mn and Si addition on microstructure and tensile properties of cold-rolled and annealed pearlite in eutectoid Fe–C alloys', *ISIJ Int.*, 2004, **44**, 171–178.
3. J. T. Wang, J. X. Huang, Z. Z. De, Z. Zhang and X. C. Zhao: 'Microstructure transformation in a pearlite steel during equal channel angular pressing', in 'Ultrafine grained materials III' (ed. Y. T. Zhu, et al.,), 673–678; 2004, Warrendale, PA, TMS.
4. L. C. Zhou, Y. H. Li, W. F. He, G. Y. He, X. F. Nie, D. L. Chen, Z. L. Lai and Z. B. An: 'Deforming TC6 titanium alloys at ultrahigh strain rates during multiple laser shock peening', *Mater. Sci. Eng. A*, 2013, **A578**, 181–186.
5. X. Wang, W. G. Xia, X. Q. Wu, Y. P. Wei and C. G. Huang: 'Microstructure and mechanical properties of an austenite NiTi shape memory alloy treated with laser induced shock', *Mater. Sci. Eng. A*, 2013, **A578**, 1–5.
6. J. Z. Lu, K. Y. Luo, Y. K. Zhang, C. Y. Cui, G. F. Sun, J. Z. Zhou, L. Zhang, J. You, K. M. Chen and J. W. Zhong: 'Grain refinement of LY2 aluminum alloy induced by ultra-high plastic strain during multiple laser shock processing impacts', *Acta Mater.*, 2010, **58**, 3984–3994.
7. X. C. Zhang, Y. K. Zhang, J. Z. Lu, F. Z. Xuan, Z. D. Wang and S. T. Tu: 'Improvement of fatigue life of Ti–6Al–4V alloy by laser shock peening', *Mater. Sci. Eng. A*, 2010, **A527**, 3411–3415.
8. J. Z. Lu, H. Qi, K. Y. Luo, M. Luo and X. N. Cheng: 'Corrosion behaviour of AISI 304 stainless steel subjected to massive laser shock peening impacts with different pulse energies', *Corros. Sci.*, 2014, **80**, 53–59.
9. H. Lim, P. Kim, H. Jeong and S. Jeong: 'Enhancement of abrasion and corrosion resistance of duplex stainless steel by laser shock peening', *J. Mater. Process. Technol.*, 2012, **212**, 1347–1354.
10. S. Sathyajith, S. Kalainathan and S. Swaroop: 'Laser peening without coating on aluminum alloy Al–6061–T6 using low energy Nd:YAG laser', *Opt. Laser Technol.*, 2013, **45**, 389–394.
11. N. Saklakoglu, S. G. Irizalp, E. Akman and A. Demir: 'Near surface modification of aluminum alloy induced by laser shock processing', *Opt. Laser Technol.*, 2014, **64**, 235–241.
12. X. D. Ren, L. Ruan, S. Q. Yuan, H. M. Yang, Q. B. Zhan, L. M. Zheng, Y. Wang and F. Z. Dai: 'Metallographic structure evolution of 6061-T651 aluminum alloy processed by laser shock peening: effect of tempering at the elevated temperatures', *Surf. Coat. Technol.*, 2013, **221**, 111–117.
13. X. D. Ren, L. Ruan, S. Q. Yuan, N. F. Ren, L. M. Zheng, Q. B. Zhan, J. Z. Zhou, H. M. Yang, Y. Wang and F. Z. Dai: 'Dislocation polymorphism transformation of 6061-T651 aluminum alloy processed by laser shock processing: effect of

tempering at the elevated temperatures', *Mater. Sci. Eng. A*, 2013, **A578**, 96–102.
14. X. D. Ren, D. W. Jiang, Y. K. Zhang, T. Zhang, H. B. Guan and X. M. Qian: 'Effects of laser shock processing on 00Cr12 mechanical properties in the temperature range from 25°C to 600°C', *Appl. Surf. Sci.*, 2010, **257**, 1712–1715.
15. C. Ye, S. Suslov, X. L. Fei and G. J. Cheng: 'Bimodal nanocrystallization of NiTi shape memory alloy by laser shock peening and post-deformation annealing', *Acta Mater.*, 2011, **59**, 7219–7227.
16. T. T. He, Y. Xiong, F. Z. Ren, Z. Q. Guo and A. A. Volinsky: 'Microstructure of ultra-fine-grained high carbon steel prepared by equal channel angular pressing', *Mater. Sci. Eng. A*, 2012, **A535**, 306–310.
17. Y. Xiong, T. T. He, Z. Q. Guo, H. Y. He, F. Z. Ren and A. A. Volinsky: 'Mechanical properties and fracture characteristics of high carbon steel after equal channel angular pressing', *Mater. Sci. Eng. A*, 2013, **A563**, 163–167.
18. C. S. Zheng, L. F. Li, W. Y. Yang and Z. Q. Sun: 'Enhancement of mechanical properties by changing microstructure in the eutectoid steel', *Mater. Sci. Eng. A*, 2012, **A558**, 158–161.
19. C. S. Zheng, L. F. Li, W. Y. Yang and Z. Q. Sun: 'Microstructure evolution and mechanical properties of eutectoid steel with ultrafine or fine (ferrite + cementite) structure', *Mater. Sci. Eng. A*, 2014, **A599**, 16–24.
20. Z. Q. Lv, P. Jiang, Z. H. Wang, W. H. Zhang, S. H. Sun and W. T. Fu: 'XRD analyses on dissolution behavior of cementite in eutectoid pearlitic steel during cold rolling', *Mater. Lett.*, 2008, **62**, 2825–2827.
21. R. Song, D. Ponge, D. Raabe and R. Kaspar: 'Microstructure and crystallographic texture of an ultrafine grained C–Mn steel and their evolution during warm deformation and annealing', *Acta Mater.*, 2005, **53**, 845–858.
22. V. G. Gavriljuk: 'Decomposition of cementite in pearlitic steel due to plastic deformation', *Mater. Sci. Eng. A*, 2003, **A345**, 81–89.
23. W. J. Nam, C. M. Bae, S. J. Oh and S. Kwon: 'Effect of interlamellar spacing on cementite dissolution during wire drawing of pearlitic steel wires', *Scr. Mater.*, 2000, **42**, 457–463.
24. Y. Xiong, S. H. Sun, Y. Li, J. Zhao, Z. Q. Lv, D. L. Zhao, Y. Z. Zheng and W. T. Fu: 'Effect of warm cross-wedge rolling on microstructure and mechanical property of high carbon steel rods', *Mater. Sci. Eng. A*, 2006, **A431**, 152–157.
25. W. T. Fu, Y. Xiong, J. Zhao, Y. Li, T. Furuhara and T. Maki: 'Microstructural evolution of pearlite in eutectoid Fe–C alloys during severe cold rolling', *J. Mater. Sci. Technol.*, 2005, **21**, 25–27.
26. X. Scherpereel, P. Peyre, R. Fabbro, G. Lederer and N. Celati: 'Modification of electrochemical properties of stainless-steel by laser shock processing', in '3rd International Meeting on Computer Methods and Experimental Measurements for Surface Treatment Effects', (ed. E. M. H Aliabadi), 83–92; 1997, England, Oxford.
27. P. Peyre and R. Fabbro: 'Laser shock processing: a review of the physics and applications', *Opt. Quantum Electron.*, 1995, **27**, 1213–1229.
28. E. J. Fasiska and H. Wagenblast: 'Dilation of alpha iron by carbon', *Trans. Metall. Soc. AIME*, 1967, **239**, 1818–1820.
29. Y. Xiong, T. T. He, Z. Q. Guo, H. Y. He, F. Z. Ren and A. A. Volinsky: 'Effects of laser shock processing on surface microstructure and mechanical properties of ultrafine-grained high carbon steel', *Mater. Sci. Eng. A*, 2013, **A570**, 82–86.
30. Q. S. Huang, L. F. Li, W. Y. Yang and Z. Q. Sun: 'Dynamic transformation of undercooling austenite and microstructure refinement in a eutectoid steel', *Acta Metall. Sinica*, 2007, **7**, 724–730.
31. W. Chen, L. F. Li, W. Y. Yang, Z. Q. Sun and J. P. He: 'Microstructure evolution of hypereutectoid steels during warm deformation. I. Formation of equiaxial ferrite and effects of Al', *Acta Metall. Sinica*, 2009, **5**, (2), 151–155.